Hybrid power plant design for low-carbon hydrogen in the United States

Journal of Physics: Conference Series **2767** (2024) 082019 doi:10.1088/1742-6596/2767/8/082019

Hybrid power plant design for low-carbon hydrogen in the United States

E Grant[1], K Brunik[1], J King[1], C E Clark[1]

[1]National Renewable Energy Laboratory, Golden, Colorado, United States

E-mail: elenya.grant@nrel.gov

Abstract.

In this study, we provide a nationwide techno-economic analysis of clean hydrogen production powered by a hybrid renewable energy plant for over 50,000 locations in the United States. We leverage the open-source Hybrid Optimization Performance Platform (HOPP) tool to simulate the hourly performance of an off-grid wind-solar plant integrated with a 1-GW polymer exchange membrane electrolyzer system. The levelized cost of hydrogen is calculated for varying technology costs, and tax credits to explore cost sensitivities independent of plant design, performance, and site selection. Our findings suggest that strategies for cost reduction include selecting sites with abundant wind resources, complementary wind and solar resources, and optimizing the sizing of wind and solar assets to maximize the hybrid plant capacity factor. These strategies are linked to increased hydrogen production and reduced electrolyzer stack replacements, thereby lowering the overall cost of hydrogen.

1. Introduction

Low-carbon hydrogen presents a unique opportunity to accelerate the expansion of renewable energy into new regions. In regions with limited renewable resources, hydrogen can act as a buffer when paired with a renewable power plant, providing a reliable energy storage solution for extended durations. Integrating hydrogen production with hybrid renewable energy plants opens up the possibility for locations previously considered unsuitable for wind energy deployment [1] due to factors such as inadequate infrastructure, expensive grid interconnection costs, or being better suited for solar energy, to become ideal candidates for off-grid hydrogen production from hybrid renewable energy plants. These plants can leverage policy incentives from the Inflation Reduction Act (IRA) [2] to expand the scope of available infrastructure while creating more flexible systems for meeting energy demands.

Past research has concentrated on low-carbon hydrogen production in the United States using single-technology systems. A techno-economic analysis evaluating off-grid wind-based hydrogen production at 1,000 locations across the country revealed that regions with abundant wind resources can produce cost-competitive low-carbon hydrogen [3]. Another study, assessing 40 locations in the United States, concluded that hydrogen produced from solar photovoltaic (PV)-powered electrolysis is projected to be cost-competitive with grid-connected electrolysis by 2050 [4]. While it is estimated that the available wind and solar resource can individually accommodate the anticipated growth in hydrogen demand [5], hydrogen produced from single-technology systems faces challenges for widespread adoption. Using hybrid plants to harness the available renewable resource, hydrogen may be produced more efficiently, reliably, and affordably.

Previous hybrid plant designs have focused on maximizing annual energy production by optimizing the layout of wind and solar assets [6]. Ongoing evidence underscores the significance of incorporating electrolyzer operation considerations in the design of renewable plants for hydrogen production [7, 8]. Electrolyzers powered by renewable energy may encounter issues such as heightened electrode degradation due to on/off cycling, failure to meet minimum operating load constraints, and delays in cold-start production [9, 10]. While some studies have explored dynamic control strategies for grid-connected electrolyzer systems to enhance revenue [11, 12], and others have looked at degradation and control strategies for renewable-powered electrolyzers [13, 7], only a few have addressed the dynamics of electrolyzers in off-grid scenarios or their influence on hybrid plant design [14, 15]. Furthermore, these studies have predominantly concentrated on single-location case studies, constraining the comprehension of site-specific characteristic impacts on plant design.

The aim of this paper is to build on previous work by addressing hydrogen losses stemming from dynamic operation of an electrolyzer system, enhancing spatial precision in location selection, and evaluating how design characteristics of a hybrid wind-solar facility impact the levelized cost of hydrogen (LCOH). Through dynamic simulations, we analyze gigawatt-scale off-grid hybrid plant configurations, including wind, solar, and electrolyzer assets, for over 50,000 sites in the United States. The paper is organized as follows: Sections 2.1 and 2.2 describe the simulation tools, component models, costs, and financial assumptions. Section 2.3 details the hybrid plant sizing method. Section 3 presents the influence of hybrid plant design on hydrogen production and key drivers for LCOH reduction. Section 4 summarizes considerations for hybrid plant design to minimize cost.

2. Methods

Hybrid plant capacity sizing simulations, encompassing both wind and PV, were conducted at 50,082 sites across the contiguous United States [16]. The chosen locations exclude protected land areas, counties with wind moratoriums, and military installations and surrounding exclusion zones (such as Risk of Adverse Impact to Military Operations and Readiness Areas) [17].

2.1. Performance Model

We use the open-source Python-based Hybrid Optimization Performance Platform (HOPP) tool [18] to simulate plant performance and calculate LCOH, considering technology costs and policy scenarios. Simulations are conducted with an hourly time resolution and a 1-year simulation length. The HOPP simulation process is outlined in Figure 1.

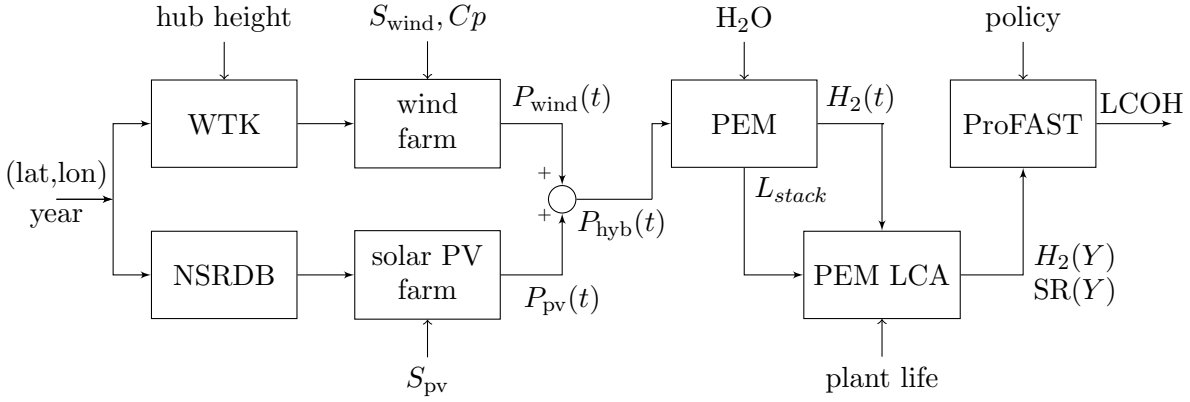

Figure 1: HOPP simulation architecture.

Site-specific wind and solar resource data for reference year 2013 are collected from the Wind Integration National Dataset Toolkit (WTK) and the National Solar Resource Database (NSRDB), respectively [19, 20]. The wind resource data accounts for the hub height of the turbine, which is set at 140 m.

To simulate wind farm performance, we use the PySAM `Windpower` module, with wind resource data, the turbine power curve C_p, and wind capacity S_{wind} as inputs [21]. We use a 6-MW reference wind turbine [22], representing wind turbine characteristics outlined in the National Renewable Energy Laboratory's 2023 Annual Technology Baseline (ATB) for all sites [23].

For the solar PV farm performance simulation, we use the PySAM `Pvwattsv8` module, requiring solar resource data and the solar DC capacity S_{pv} as inputs [21]. The solar farm comprises utility-scale, single-axis tracking PV panels with a rotational limit of 45 degrees, corresponding to the `PVWattsSingleOwner` default configuration [24].

The hybrid plant generation profile, $P_{\text{hyb}}(t)$, is a sum of the hourly wind $P_{\text{wind}}(t)$ and PV generation profiles $P_{\text{pv}}(t)$ output from PySAM. Energy from the hybrid plant is converted to hydrogen $H_2(t)$ through polymer exchange membrane (PEM) electrolysis. Each site has a 1-GW installed electrolyzer system, comprising 100 stacks rated at 10 MW. Input power is distributed amongst the stacks using a baseline equal power-split control method [7].

The PEM electrolyzer is modeled at the cell level using first-principle equations, with detailed information available in [25, 3]. It initiates operation with a beginning-of-life (BOL) rated efficiency, of 54.61 kWh/kg-H_2. Short-term hydrogen losses occur when a stack is turned on due to a 10-min warm-up delay in which no hydrogen is produced, but power is consumed. Long-term hydrogen losses are a result of cell degradation, d_{cell}, from steady operation, on-off switching, and fatigue cycling. The percent change in efficiency from BOL performance, $\Delta\eta$, resulting from cell degradation, $d_{cell}(t)$, is given by Equation 1. The actual hydrogen produced when the cell is degraded, $m_{H_2}(t)$, is given by Equation 2:

$$1 + \Delta\eta = \frac{V_{cell,BOL} + d_{cell}(t)}{V_{cell,BOL}} \tag{1}$$

$$m_{H_2}(t) = \frac{m_{H_2,BOL}}{1 + \Delta\eta} \tag{2}$$

where $V_{cell,BOL}$ is the BOL (or un-degraded) cell voltage, and $m_{H_2,BOL}$ is the BOL hydrogen production.

In the first year of operation, the electrolyzer system produces more hydrogen than subsequent years because the stacks degrade at different rates and may not be replaced simultaneously. To account for the long-term impact of degradation, the model conducts a life-cycle assessment of the annual hydrogen production, $H_2(Y)$, and stack replacement schedule, SR(Y), for each year, Y, of the plant's life. The stack life, L_{stack}, can be estimated from the cell degradation at the end of the simulation, $d_{cell}(t_{sim})$, and the number of hours the stack was operational, t_{ON}, and given by Equation 3:

$$L_{stack} = \frac{d_{cell}(t_{sim})}{d_{cell,EOL}} t_{ON} \tag{3}$$

where $d_{cell,EOL}$ is the end-of-life (EOL) degradation voltage, corresponding to a 10% efficiency loss from the BOL [26]. When $d_{cell}(t) = d_{cell,EOL}$, the stack is replaced and the degradation returns to zero [11].

2.2. Cost Model

The LCOH is similar to a break-even price and represents the ratio of the net present costs of the plant to the net present hydrogen produced over the plant's lifetime. A simplified calculation

of the LCOH is given by Equation 4:

$$\text{LCOH [\$/kg]} \approx \sum_{Y=0}^{PL} \sum_{k} \frac{C_{k,Y}}{(1+DR)^Y} / \sum_{Y=0}^{PL} \frac{H_2(Y)}{(1+DR)^Y} \tag{4}$$

where $C_{k,Y}$ is the cost for a component k in year Y, PL is the 30-year plant life, and DR is the discount rate. The LCOH represents an off-grid hybrid renewable energy plant integrated with a hydrogen production facility. Therefore, the costs associated with the wind and solar assets are included as capital and operational expenditures (CapEx and OpEx). The capital cost is only paid in the first year, whereas feedstock costs, fixed and variable operating costs, and component replacement costs (if needed), are paid every year. We use the Production Financial Analysis Scenario Tool (ProFAST) to calculate LCOH which includes the parameters used in Equation 4 and additional financial parameters outlined in Table 3 [27].

2.2.1. Tax Credits The IRA includes tax provisions for renewable energy projects, such as a production tax credit (PTC) and an investment tax credit (ITC) for clean electricity and clean hydrogen[2]. In this study, we calculate the LCOH under two scenarios: one incorporating maximum policy support (Maximum Policy) and the other without any policy incentives (No Policy). Under the Maximum Policy scenario, we consider the application of a 50% ITC to solar and hydrogen storage assets, which includes the 30% base credit, the 10% domestic content bonus credit, and the 10% energy community bonus credit, as specified by Section 48 and 48E. Additionally, a \$0.03/kWh PTC is applied to wind energy production, which includes \$0.027/kWh for meeting labor requirements plus a \$0.003/kWh bonus credit from either the energy community bonus or domestic content bonus, as specified by Section 45 and 45Y. Furthermore, a \$3/kg-H_2 PTC is applied for clean hydrogen production, as specified by Section 45 and 45V.

2.2.2. System Costs We obtain wind and PV cost projections for 2030 from the National Renewable Energy Laboratory's 2023 ATB [23], as presented in Table 1. The ATB categorizes future costs into three technology innovation scenarios: Conservative, Moderate, and Advanced. Costs for utility PV are provided in \$/kW_{AC}, and we convert them to \$/kW_{DC} using a DC-to-AC ratio of 1.34. The electrolyzer overnight CapEx includes a 12% installation factor and 42% indirect costs [28, 29]. Table 2 includes additional electrolyzer system costs and assumptions [30, 28]. Other financial parameters used in cash flow modeling are provided in Table 3.

Table 1: 2030 costs for each technology cost scenario (reported in 2021\$).

	Conservative	Moderate	Advanced
Land-Based Wind CapEx [\$/kW]	1265	1139	1084
Land-Based Wind OpEx [\$/kW-year]	29	27	23
Utility-Scale PV CapEx [\$/kW_{DC}]	884.33	774.03	641.79
Utility-Scale PV OpEx [\$/kW_{DC}-year]	14.93	12.69	11.94
PEM Electrolyzer Overnight CapEx [\$/kW]	720.45	540.74	270.37

2.3. Hybrid Plant Sizing Method

The wind and solar capacities, S_{wind} and S_{pv}, are sized to produce the lowest (or near lowest) LCOH, using a heuristic-based approach for reduced computation time, minimized complexity, increased usability and accessibility, and flexibility across financial parameters, cost scenarios,

Table 2: Electrolyzer costs and assumptions.

Parameter	Value
Fixed OpEx [$/kW-year]	12.8
Variable OpEx [$/MWh]	1.3
Stack Replacement Cost	15% CapEx
Maximum Stack Life	77,600 hours
Water Cost	0.004 [$/gal]
Water Usage	10 kg H_2O/kg-H_2

Table 3: Financial assumptions

Parameter	Value
Debt/Equity	1.72
Discount Rate	9.48%
Debt Interest Rate	4.6%
Income Tax Rate	25.74%
Capital Gains Tax Rate	15%
Installation Period	3 years

and locations. This study aims to identify trends that arise between electrolyzer performance, plant design, and LCOH and use these insights to enhance the sizing methodology for subsequent analyses. The method described in this section is the initial iteration of this design approach, and a comprehensive description of the optimization method is omitted for brevity.

At each site, we run a parametric sweep of $n = 36$ hybrid plant designs, following the process outlined in Figure 1 for each iteration, i. For each generation technology (wind and solar), we test 6 capacity multipliers, relative to the electrolyzer capacity. These multiplier values – 1/4, 1/2, 1, 4/3, 5/3 and 2 – are intended to sweep a large combination of possible designs, resulting in 36 distinct designs. To enhance computational efficiency, we model the electrolyzer system as a single stack rated at 1 GW during the sizing optimization. For each combination of wind, $x[i]$, and PV, $y[i]$, capacity, we calculate the Moderate - No Policy LCOH, $C[i]$.

We approximate the LCOH as a function of wind and PV capacity $f(x, y)$ and solve for the curve coefficients using data from the parametric sweep. The optimal wind and PV capacities, x_* and y_*, are solved for by setting the partial derivatives, $\frac{\partial f}{\partial x}$ and $\frac{\partial f}{\partial y}$ to zero. Using the approximated LCOH function $f(x, y)$, we estimate the LCOH for the *estimated optimal* wind and PV capacities, x_* and y_*. The *estimated minimum LCOH* $f(x_*, y_*)$ is then compared to the *calculated minimum LCOH* from the initial parametric sweep, $C[i_*]$, as given by Equation (5):

$$S_{\text{wind}}, S_{\text{pv}} = \begin{cases} x[i_*], y[i_*] & \text{if } f(x_*, y_*) \geq C[i_*] \\ x_*, y_* & \text{if } f(x_*, y_*) < C[i_*] \end{cases} \tag{5}$$

where $S_{\text{wind}}, S_{\text{pv}}$ are the final wind and PV capacities. We refer to the case where $S_{\text{wind}}, S_{\text{pv}} = x_*, y_*$ as the *estimated plant design* corresponding to the heuristic sizing approach. Whereas the case $S_{\text{wind}}, S_{\text{pv}} = x[i_*], y[i_*]$ is described as *plant design from the parametric sweep.*

3. Results

This section presents pathways for cost reduction in low-carbon hydrogen production from an off-grid hybrid renewable energy plant. We begin with a sensitivity study on LCOH in Section 3.1. Section 3.2 examines the potential of leveraging hybrid plant design and site selection for cost minimization. Building on this, Section 3.3 considers the role of electrolyzer performance and hybrid plant design for further cost reduction opportunities.

3.1. Technology Costs and Tax Credits

Figure 2 shows the LCOH of 50,082 sites across the United States; grey areas in the figure are locations with either wind moratoriums or military installations [17]. Each subfigure represents a different technology cost scenario and policy scenario. The reduction in technology costs leads to a consecutive decrease in the national average LCOH by over $0.60/kg-$H_2$ for each scenario. Under the Maximum Policy scenario, the average LCOH sees an additional reduction

of over \$4/kg-H_2 compared to the No Policy scenario. A negative LCOH occurs when the clean electricity and hydrogen PTCs exceed the cost to produce hydrogen.

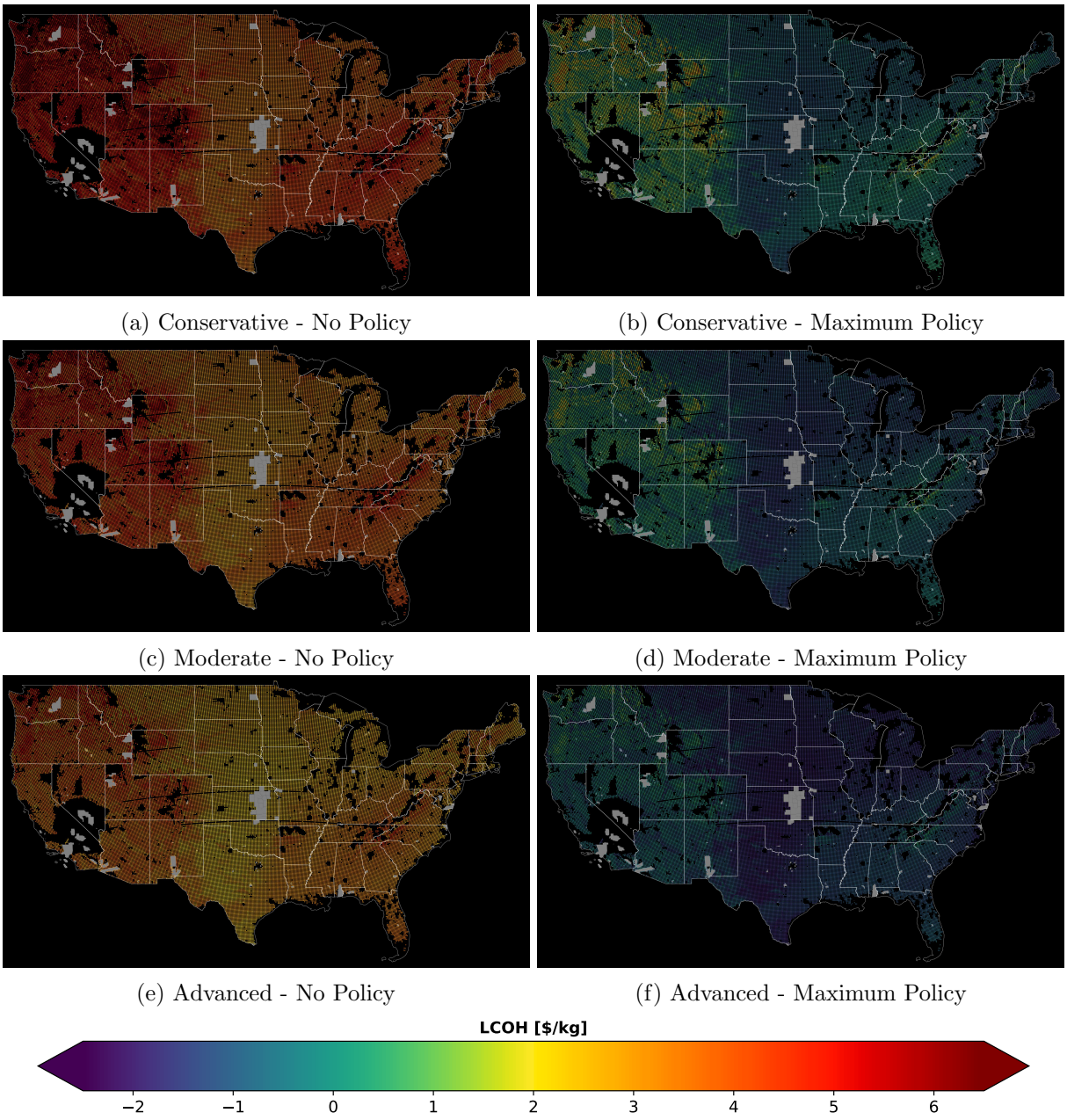

(a) Conservative - No Policy

(b) Conservative - Maximum Policy

(c) Moderate - No Policy

(d) Moderate - Maximum Policy

(e) Advanced - No Policy

(f) Advanced - Maximum Policy

Figure 2: U.S. map of LCOH (\$/kg-H_2) across the Conservative, Moderate, and Advanced technology scenarios and No Policy and Maximum Policy scenarios for 2030.

3.2. Hybrid Plant Design and Site Selection

Figure 3 shows the relationships among site-specific characteristics, hybrid plant design, and its impact on LCOH. The figure shows the LCOH for the Moderate - No Policy scenario. The hybrid plant design is described by the total hybrid plant capacity, S_{hyb}, where $S_{\text{hyb}} = S_{\text{wind}} + S_{\text{pv}}$, and the wind capacity fraction, $S_{\text{wind}}/S_{\text{hyb}}$ (i.e. the ratio wind capacity to the total hybrid plant

capacity).

Individual technology capacity factors can be used as a metric to assess resource availability at a given location. Figure 3b indicates that the estimated plant design typically incorporates more wind capacity for sites with low PV capacity factors, but there is not a direct correlation between LCOH and PV capacity factor. In Figure 3a, locations with higher wind capacity factors have a lower LCOH, which is consistent with the findings of [3].

Figure 3d shows that increased resource complementarity generally results in a lower LCOH. Wind and solar resource complementarity is represented by the hourly Pearson correlation coefficient [31]. A lower (or more negative) correlation coefficient indicates a more complementary wind and solar resource [31].

In Figure 3, the horizontal lines indicate instances where the plant design from the parametric sweep was selected instead of the estimated plant design, representing 43% of the locations. The estimated plant designs, shown by the purple data cluster in Figure 3c, have a substantially larger hybrid plant capacity, S_{hyb}, than the plant designs from the parametric sweep. These results suggest that the sizing methodology requires further development to avoid oversizing the hybrid plant. However, the general trend is promising, as the $S_{\text{wind}}/S_{\text{hyb}}$ decreases for locations with lower wind capacity factors and increases with lower PV capacity factors.

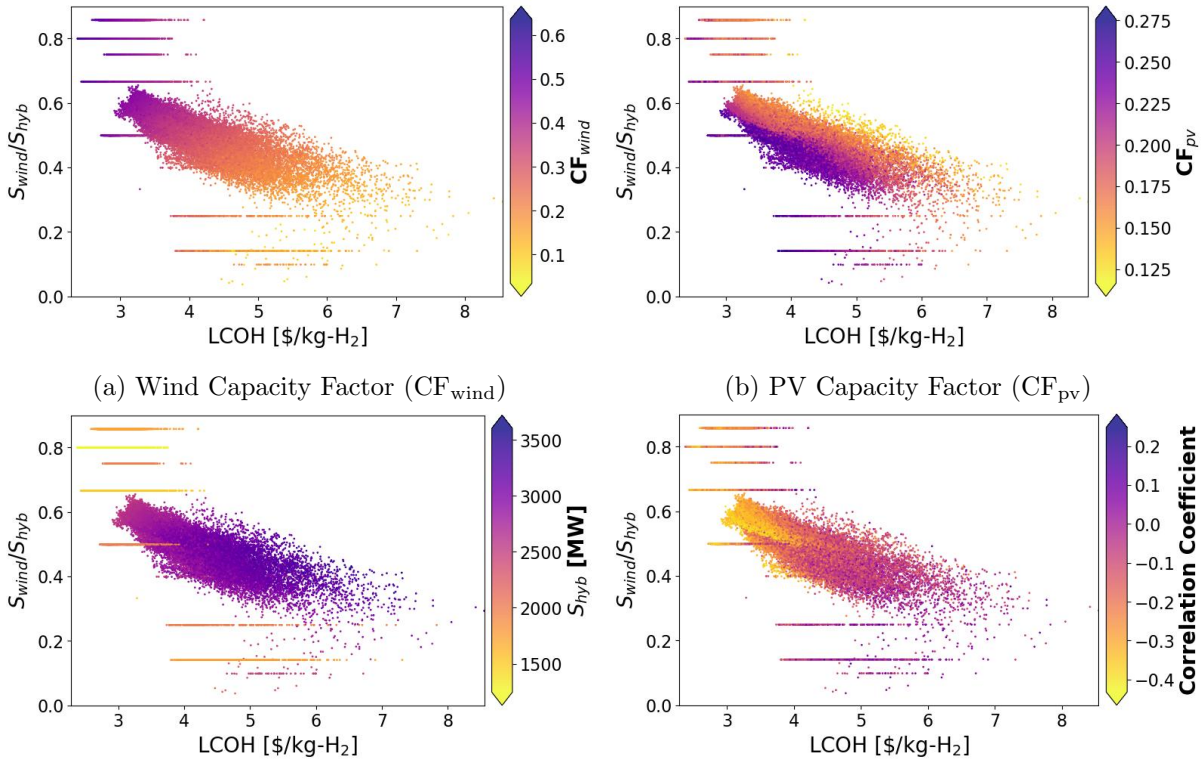

(a) Wind Capacity Factor (CF_{wind})

(b) PV Capacity Factor (CF_{pv})

(c) Hybrid Plant Capacity (S_{hyb})

(d) Wind and Solar Resource Complementarity

Figure 3: Relationship of LCOH and wind capacity fraction ($S_{\text{wind}}/S_{\text{hyb}}$) to wind capacity factor, PV capacity factor, hybrid plant capacity, and resource complementarity, which are represented as a color scale.

3.3. Hybrid Plant Performance and Electrolyzer Operation

To leverage hybrid plant design as a cost reduction mechanism, it is important to understand its impact on electrolyzer operation and the sensitivity of LCOH to electrolyzer performance.

The results in this section use the LCOH for the Moderate - No Policy scenario.

In Figure 4, we observe the correlation between LCOH and electrolyzer performance (Figure 4a) as well as hybrid plant performance (Figure 4b). The electrolyzer capacity factor is calculated as the mean annual hydrogen production, $H_2(Y)$, divided by the maximum annual hydrogen production based on the BOL efficiency. From Equation 4, we see that LCOH decreases with an increase in hydrogen production. Stack life provides insight to the hydrogen losses, encompassing short-term and long-term losses from dynamic operation. When a stack is turned on, it has short-term hydrogen losses from the warm-up delay and accumulates long-term hydrogen losses from degradation associated with on/off switching. A shorter stack life indicates more frequent on/off switching, causing hydrogen losses and reducing the electrolyzer capacity factor, thereby increasing LCOH. Additionally, stack replacements cost 15% of the electrolyzer overnight capital cost and more frequent replacements contribute to a higher LCOH. Designing the hybrid plant and electrolyzer operation to minimize hydrogen losses and maximize stack life is essential for achieving a lower LCOH.

As the hybrid plant capacity factor, $\mathrm{CF_{hyb}}$, increases, the LCOH decreases, as shown in Figure 4b. The hybrid capacity factor represents a combination of the individual component capacity factors weighted by the corresponding component capacities, given by Equation (6):

$$\mathrm{CF_{hyb}} = \frac{\mathrm{CF_{wind}} S_{\mathrm{wind}} + \mathrm{CF_{pv}} S_{\mathrm{pv}}}{S_{\mathrm{wind}} + S_{\mathrm{pv}}} \tag{6}$$

The hybrid capacity factor is strongly driven by the wind capacity factor, illustrated by similar trends in Figure 3a and Figure 4b. In Figure 5, the electrolyzer performance is shown, influenced

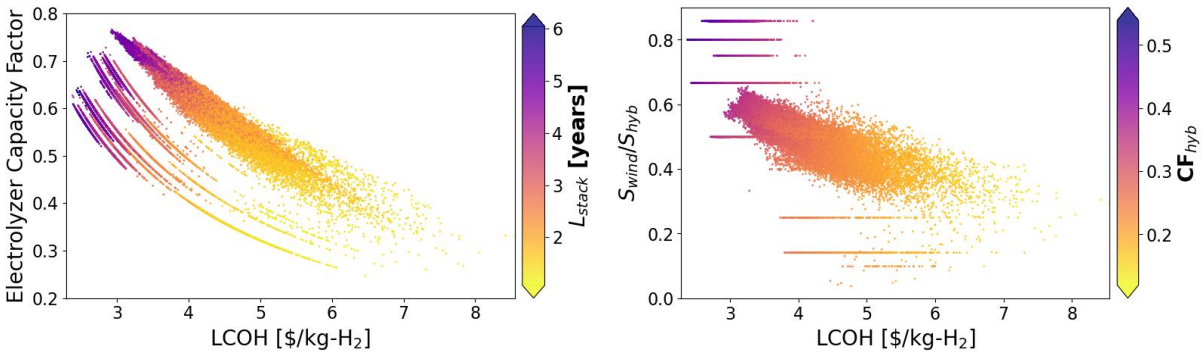

(a) Hydrogen losses are reflected in the electrolyzer capacity factor and stack life (L_{stack}).

(b) Plant design is represented by the wind capacity fraction ($S_{\mathrm{wind}}/S_{\mathrm{hyb}}$) and hybrid capacity factor ($\mathrm{CF_{hyb}}$).

Figure 4: Relationship of the LCOH to hydrogen losses and hybrid plant design.

by hybrid plant performance (Figure 5a) and site-specific characteristics (Figure 5b). Plant designs with a $\mathrm{CF_{hyb}} \geq 0.374$ have an average LCOH of \$2.88/kg-H_2, stack life of 4.3 years, and electrolyzer capacity factor of 0.59. Conversely, plant designs with a $\mathrm{CF_{hyb}} < 0.374$ have an average LCOH of \$3.68/kg-H_2, stack life of 2.8 years, and electrolyzer capacity factor of 0.49. Therefore, choosing wind and PV capacities to maximize the $\mathrm{CF_{hyb}}$ in Equation (6) is likely to result in lower-cost hydrogen. The highest PV capacity factor is 0.26, such that achieving $\mathrm{CF_{hyb}} \geq 0.374$ would require the site to have a wind capacity factor of $\mathrm{CF_{wind}} \geq 0.374$.

The relationship between LCOH, resource complementarity, and stack life (Figure 5b) mirrors that of LCOH, resource complementarity, and the wind capacity fraction (Figure 3d). All locations with a stack life above 4 years have a negative correlation coefficient and an LCOH

below \$3.85/kg-H_2. When the stack life is below 4 years, the average LCOH is \$4/kg-H_2. When the stack life is above 4 years, the average LCOH is \$3/kg-H_2. Locations with complementary resources are best to ensure a longer stack life and therefore a lower LCOH. Note that the streaks observed in Figure 4a and Figure 5a correspond to the horizontal lines seen in Figure 3 and Figure 4b.

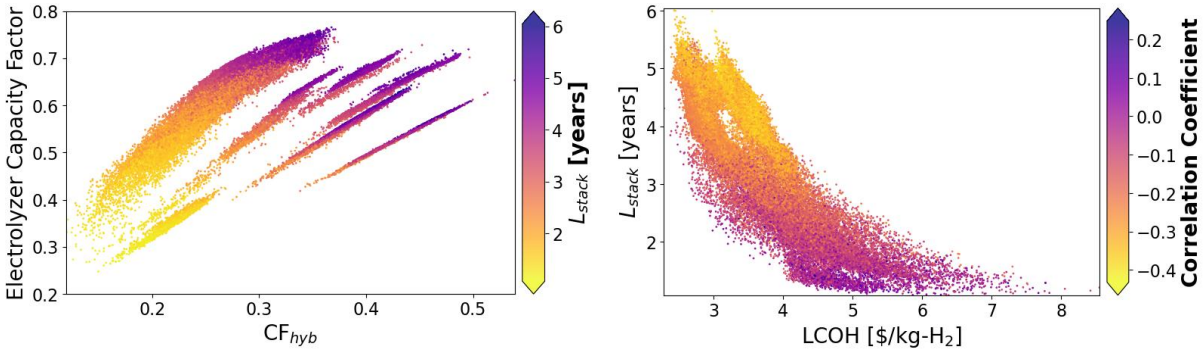

(a) Hybrid Plant design and performance are reflected in the hybrid capacity factor (CF_{hyb}).

(b) Resource complementarity is represented with the hourly Pearson correlation coefficient.

Figure 5: Relationship of hydrogen losses to the hybrid plant design and performance (left). Relationship of LCOH (Moderate - No Policy) to stack life (L_{stack}) and resource complementarity (right).

4. Conclusion

This paper explores various pathways to reduce costs in off-grid renewable-powered electrolysis. We found that lower LCOH values correspond to a higher electrolyzer capacity factor and longer stack life, representing reduced hydrogen losses and costs related to dynamic electrolyzer operation. Hybrid plant designs minimizing hydrogen losses and having a higher hybrid capacity factor contribute to a lower LCOH. Locations with complementary resources and a higher hybrid capacity factor experience fewer hydrogen losses and longer stack life. In areas with non-complementary resources and limited wind availability, advanced electrolyzer control strategies or adding a battery can mitigate hydrogen losses. Besides plant design and location selection, eligibility for tax credits further reduces the LCOH, making these low-carbon hydrogen systems cost competitive in the near future. Future work will expand the modeling framework presented in this paper to various hydrogen end uses, including hydrogen transmission and bulk storage in the system costs. Other considerations for future work include validating and building upon the hybrid plant sizing methodology, including electrolyzer capacity as a design variable, and exploring the LCOH for grid-connected hybrid plants and single-technology plants.

Acknowledgements

This work was authored by the National Renewable Energy Laboratory, operated by Alliance for Sustainable Energy, LLC, for the U.S. Department of Energy (DOE) under Contract No. DE-AC36-08GO28308. Funding provided by the U.S. Department of Energy Office of Energy Efficiency and Renewable Energy Wind Energy Technologies Office and Hydrogen and Fuel Cell Technologies Office. The views expressed in the article do not necessarily represent the views of the DOE or the U.S. Government. The U.S. Government retains and the publisher, by accepting the article for publication, acknowledges that the U.S. Government retains a nonexclusive, paid-up, irrevocable, worldwide license to publish or reproduce the published form of this work, or allow others to do so, for U.S. Government purposes.

References

[1] Wiser R, Bolinger M, Hoen B, Millstein D, Rand J, Barbose G, Darghouth N, Gorman W, Jeong S, O'Shaughnessy E and Paulos B 2023 URL https://www.osti.gov/biblio/1996790
[2] Yarmuth J A 2022 Text - H.R.5376 - 117th Congress (2021-2022): Inflation Reduction Act of 2022 archive Location: 2021/2022 URL http://www.congress.gov/
[3] Clark C E, Barker A, Brunik K, Kotarbinski M, Grant E, Roberts O, King J, Stanley A P, Bhaskar P and Bay C 2023 *Energy Conversion and Management* **296** 117595 URL https://doi.org/10.1016/j.enconman.2023.117595
[4] Xi W, Boyd M, Ruth M and Kurup P 2023 URL https://doi.org/10.2172/1961147
[5] Connelly E, Penev M, Milbrandt A, Roberts B, Gilroy N and Melaina M 2020 URL https://www.osti.gov/biblio/1660128
[6] Tripp C, Guittet D, King J and Barker A 2022 *Wind Energy Science* **7** 697–713 URL https://doi.org/10.5194/wes-7-697-2022
[7] Tully Z, Starke G, Johnson K and King J 2023 *IEEE Conference on Control Technology and Applications (CCTA)* 817–822 URL https://www.osti.gov/biblio/2203523
[8] Mehta M, Zaaijer M and Terzi D V 2022 *Journal of Physics: Conference Series* **2265** 042061 URL https://iopscience.iop.org/article/10.1088/1742-6596/2265/4/042061
[9] Ursúa A, Barrios E L, Pascual J, San Martín I and Sanchis P 2016 *International Journal of Hydrogen Energy* **41** 12852–12861 URL https://doi.org/10.1016/j.ijhydene.2016.06.071
[10] Brauns J and Turek T 2020 *Processes* **8** URL https://www.mdpi.com/2227-9717/8/2/248
[11] Matute G, Yusta J, Beyza J and Correas L 2021 *International Journal of Hydrogen Energy* **46** 1449–1460 URL https://doi.org/10.1016/j.ijhydene.2020.10.019
[12] Zheng Y, You S, Bindner H W and Münster M 2022 *Applied Energy* **307** 118091 URL https://doi.org/10.1016/j.apenergy.2021.118091
[13] Brauns J and Turek T 2022 *Electrochimica Acta* **404** 139715 URL https://doi.org/10.1016/j.electacta.2021.139715
[14] Ginsberg M J, Esposito D V and Fthenakis V M 2023 *Cell Reports Physical Science* **4** 101625 URL https://doi.org/10.1016/j.xcrp.2023.101625
[15] Su W, Zheng W, Li Q, Yu Z, Han Y and Bai Z 2023 *Frontiers in Energy Research* **11** URL https://www.frontiersin.org/articles/10.3389/fenrg.2023.1256463
[16] Maclaurin G, Grue N, Lopez A, Heimiller D, Rossol M, Buster G and Williams T 2019 URL https://www.osti.gov/biblio/1563140
[17] Lopez A, Levine A, Carey J and Mangan C 2022 U.S. Wind Siting Regulation and Zoning Ordinances DOE/34877 URL https://data.openei.org/submissions/5733
[18] Tripp C E, Guittet D, Barker A, King J and Hamilton B 2019 Hybrid optimization and performance platform (hopp) [Computer Software] https://doi.org/10.11578/dc.20210326.1
[19] Hodge B M 2016 URL https://www.osti.gov/biblio/1247462
[20] Sengupta M, Xie Y, Lopez A, Habte A, Maclaurin G and Shelby J 2018 *Renewable and Sustainable Energy Reviews* **89** 51–60 URL https://doi.org/10.1016/j.rser.2018.03.003
[21] National Renewable Energy Laboratory PySAM URL https://sam.nrel.gov/software-development-kit-sdk/pysam.html
[22] Duffy P 2023 2023 nrel bespoke 6mw 196 URL https://github.com/NREL/turbine-models/blob/master/Onshore/2023NREL_Bespoke_6MW_196.csv
[23] National Renewable Energy Lab 2023 2023 Annual Technology Baseline URL https://atb.nrel.gov/
[24] Freeman J, Jorgenson J, Gilman P and Ferguson T 2014 URL https://www.osti.gov/biblio/1150800
[25] Grant E 2024 Baseline electrolyzer reference-design tool (bert) (in preparation)
[26] Hydrogen and Fuel Cell Technologies Office 2022 Technical targets for proton exchange membrane electrolysis URL https://www.energy.gov/eere/fuelcells/technical-targets-proton-exchange-membrane-electrolysis
[27] Kee J and Penev M 2023 Profast (production financial analysis scenario tool) [swr-23-88] [Computer Software] https://doi.org/10.11578/dc.20231211.1
[28] Peterson D, Vickers J and DeSantis D 2020 URL https://www.hydrogen.energy.gov/docs/hydrogenprogramlibraries/pdfs/19009_h2_production_cost_pem_electrolysis_2019.pdf
[29] Reznicek E *et al.* 2024 Techno-economic analysis of low-carbon hydrogen production pathways for decarbonizing steel and ammonia production (Submitted to Joule)
[30] Hunter C A, Penev M M, Reznicek E P, Eichman J, Rustagi N and Baldwin S F 2021 *Joule* **5** 2077–2101 URL https://doi.org/10.1016/j.joule.2021.06.018
[31] Harrison-Atlas D, Murphy C, Schleifer A and Grue N 2022 *Renewable Energy* **201** 111–123 URL https://doi.org/10.1016/j.renene.2022.10.060